Civil Engineering Infrastructures Journal, 52(2): 349 – 363, December2019
Print ISSN: 2322-2093; Online ISSN: 2423-6691
DOI: 10.22059/ceij.2019.277143.1557

Flexural Behavior of Lightweight Concrete Beams Reinforced with GFRP Bars and Effects of the Added Micro and Macro Fiber

Vakili, S.E.[1], Homami, P.[2*] and Esfahani, M.R.[3]

[1] Ph.D. Student, Engineering Faculty, Kharazmi University, Tehran, Iran.
[2]Assistant Professor, Engineering Faculty, Kharazmi University, Tehran, Iran.
[3] Professor, Department of Civil Engineering, Ferdowsi University of Mashhad, Mashhad, Iran.

Received: 02 Mar. 2019; Revised: 18 Aug. 2019; Accepted: 18 Aug. 2019

ABSTRACT: This study evaluated the effect of macro steel fiber (SF), micro glass fiber (GF) and micro polypropylene fiber (PF) in lightweight aggregate concrete, (LWAC) beams reinforced with glass fiber reinforced polymer (GFRP) bars. Firstly, concrete mixtures with different volume fractions of GF, PF and SF were tested up to compressive strength, then determine the optimum fiber content GF, PF and SF added into LWAC mix by 0.3%, 0.8% and 0.25% by the volume of concrete, respectively. Meanwhile, eight rectangular cross-section beams with 100 mm (width) × 200 mm (depth) × 1500 mm (length) were tested by four-point bending beam test up to the ultimate load. The GFRP bars were used to reinforce all beams. The failure modes, load-deflection behavior, ductility, flexural capacity and energy absorption were compared in the test results. The experimental results shown added fibers into LWAC improved the flexural capacity, ductility and energy absorption also enhanced moment capacity by 10.07% to 110%. The results indicated that failure modes of GF and PF specimens were in good consistency with the ACI 440.1R-06 predicted failure modes, but for SF specimens, only concrete crushing failure modes accrued. At the end step, the correction factor (Ψ) obtained from calculated of the experimental results with the flexural capacity according to the ACI 440.1R-06 and ISIS design manual No. 3.

Keywords: GFRP Bar, Lightweight Aggregate Concrete, Macro Steel Fiber, Micro Glass Fiber, Micro Polypropylene Fiber.

INTRODUCTION

The two main factors that can be used to stabilize concrete structures against earthquake and corrosion are the use of lightweight aggregate concrete (LWAC) and glass fiber reinforced polymers (GFRP) bars in concrete structures. Recently, FRP composite materials-polymeric resin-embedded fibers- have become an alternative for reinforced concrete with steel fiber. Considering non-corrosive and non-magnetic properties of FRP materials, in FRP-reinforced concrete, the problems of steel bar corrosion and electromagnetic interference can be prevented. (ACI Committee 440, 2006, Tang et al., 2006; Kara et al., 2015; Vakili et al., 2019).

Considering the numerous excellent advantages of LWAC (density between 1120 and 1920 kg/m^3 according to ACI 213R-03) more attention has been paid to its

* Corresponding author E-mail: homami@khu.ac.ir

propagation (Shafigh et al., 2011; Tajra et al., 2019). The LWAC is effectively utilized in the civil engineering field during many years, LWAC involves many desired properties including good fire resistance, upper thermal insulation, good durability, reduced density and upper seismic resistance compared with conventional concrete (Bilodeau et al., 2004; Bogas and Gomes, 2015; Oktay et al., 2015; Guler., 2018; Yoon, 2019).

Adding fibers to LWAC is improving the compressive strength and toughness (Libre et al., 2011). Addition of fiber to the LWAC significantly increments its impact insistence, post-cracking ductility and tensile strength and the effectiveness of high performance polypropylene fibers on post-peak behavior were higher than its effectiveness on pre-peak behavior (Qian et al., 2000; Hamoush et al., 2010; Choi et al., 2014; Khaloo et al., 2014).

An effective method to prevail the large crack width in concrete beams reinforced with (FRP) bars is adding of SF in tension zone. Adding of SF decreases the workability and increases the density of plain LWAC. Incidentally, the interfacial transition zone (ITZ) between cement paste and aggregates is not the weakest link in SF reinforced LWAC (SFLWAC) (Zhu et al., 2016; Badogiannis et al., 2019; Wu et al., 2019). The capacity of energy absorption is increased by increasing the volume fraction of the fibers (Lee et al., 2017). Among the different types of fibers, SF or PF were widely applied (Campione et al., 2004; Chen et al., 2005; Domagała et al., 2011).

This study focuses on the effects of the GF, PF and SF on the flexural capacity, energy absorption, ultimate load carrying and failure mode of the beam made with LWAC and reinforced with GFRP bar.

EXPERIMENTAL PROGRAM

Materials

The cement used in this study was 1-325 Portland cement composed ISIRI N.389 (ISIRI, 2000), having a specific gravity of 3.15 g/cm^3. The mechanical and physical properties of the cement have been shown in Table 1. Chemical analysis of the cement is presented in Table 2. Micro-silica utilized in this work involved an apparent density of 2,200 kg/m^3, the specific surface area of 2,800 cm^2/g. The chemical analysis of silica fume is provided in Table 3. Figure 1 shows the lightweight expanded clay aggregate (LECA) utilized in this work and Table 4 represents its chemical composition. Table 5 lists the properties of these aggregates. Properties of GF, PF and SF (Figure 2) provided by the manufacturer are represented in Table 6. Fine aggregate included crushed sand with a nominal maximum size of 5.0 mm and a bulk density of 1560 kg/m^3. The flexural reinforcement was provided by GFRP bars (Figure 3) and their material properties were delivered by the manufacturer (Table 7) and Table 8 shows the material properties of the steel bars. A naphthalene type super plasticizer was used in all mixtures to obtain sufficient fluidity in GFLWAC, PFLWAC and SFLWAC mixtures.

Table 1. Mechanical and physical properties of cement

Specific surface area (cm^2/g)	Water requirement of normal consistency (%)	Setting time (min)		Compressive strength (MPa)			Expansion of cement (%)
		Initial	Final	3d	7d	28d	
3482	25.5	183	203	32.5	40	49.6	0.03

Table 2. Chemical analysis of cement

Chemical combination	SiO_2	Al_2O_3	Fe_2O_3	CaO	MgO	SO_3	Na_2O	K_2O	Cl	C_4Af	C_3A	C_3S	C_2S
Quantity available in sample (%)	21.4	4.2	3.87	63.8	1.94	2.31	0.32	0.65	0.024	20.94	4.59	63.68	11.36

Table 3. Chemical analysis of silica fume

Chemical combination	SiC	Al_2O_3	Fe_2O_3	CaO	MgO	SO_3	Na_2O	K_2O	Cl	C	P_2O_2	SiO_2
Percent constituent (%)	0.53	1.32	0.87	0.49	0.97	0.1	0.31	1.01	0.04	0.34	0.16	93.86

Al_2O_3: Aluminum Oxide

Fig. 1. Light expanded clay aggregate (LECA)

Table 4. Chemical analysis of light expanded clay aggregate (LECA)

Chemical combination	SiO_2	Al_2O_3	Fe_2O_3	CaO	MgO	TiO_2	P_2O_5	MnO	SiO_3	Na_2O	K_2O
Percent constituent (%)	66.05	16.57	7.1	2.46	1.99	0.78	0.21	0.09	0.03	0.69	2.69

Table 5. Properties of aggregates

Aggregates	Size (mm)	Apparent density (kg/m^3)	Water absorption (%)	
			1 h	24 h
Light Expanded Clay Aggregate (LECA)	1.0- 9.50	1300	8.60	11.10
Sand	0.15- 4.75	2660	0.35	0.80

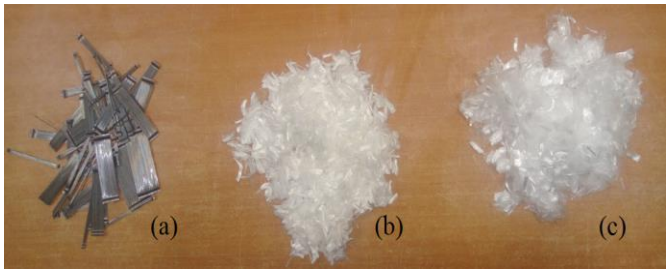

Fig. 2. Fibers used in this study: a) macro fiber steel, b) micro fiber polypropylene, and c) micro fiber glass

Table 6. Properties of fibers

Fiber type	Length (mm)	Diameter (mm)	Aspect ratio (l/d)	Density (g/cm^3)	Tensile strength (GPa)	Geometry
Steel	60	0.9	66.66	7.85	3	End hooked
Polypropylene	12	0.023	521.7	0.91	0.4	Fibrillated
Glass	15	0.019	789.47	2.6	1.5	Fibrillated

Fig. 3. GFRP bars used in this study

Table 7. Material properties of the GFRP bars

Type	Diameter (mm)	A (mm^2)	E_L (GPa)	F_1 (kN)	F_2 (kN)	ε_1 (mm)	ε_2 (mm)
GFRP	8	50.24	49.4	30.02	12	10.38×10^{-3}	3.04×10^{-3}
GFRP	10	78.50	51	33.17	11.92	11.277×10^{-3}	2.98×10^{-3}

A: is cross-sectional area of specimen, E_L: is axial (longitudinal) modulus of elasticity, F_1 and ε_1: are load and corresponding strain, respectively, F_2 and ε_2: are load and corresponding strain, respectively, at approximately 20% of the ultimate tensile capacity.

Table 8. Material properties of the steel bars

Type	Diameter (mm)	Area (mm^2)	E_L (GPa)	F_y (MP)	F_u (MPa)
Steel	6	28.26	200	300	500
Steel	8	50.24	200	300	500

A: is cross-sectional area of specimen, E_L: is axial (longitudinal) modulus of elasticity, F_y: is yield strength of the steel bars and F_u: is ultimate tensile strength of the steel bars.

Mixture Proportions and Production

In this study, the use of V_{GF} = 0.2%, 0.25% and 0.3% (GF at 0.2%, 0.25% and 0.3% by volume of the concrete), V_{PF} = 0.6%, 0.7% and 0.8% also V_{SF} = 0.15%, 0.2% and 0.25% into the LWC were tested up to the ultimate compressive strength. Then the prior determined optimum fiber content GF, PF and SF were added into the LWC mix by 0.3%, 0.8% and 0.25% by the volume of concrete, respectively; and is shown in Table 9. The method of mixing LWAC was performed by first the dry aggregate to the mixer and mixing it for 60 sec. Then, total super plasticizer plus half the water were combined and added into the mixture and continued to mix for 60 sec. Then, the cement was added to one-third of the fiber and the silica fume was mixed with half of the water and turned into a gel. Afterward, adding it into the mixture, mixing was continued for 3 min. Finally, adding the rest of the fibers to the mixture, mixing was done for 2 min.

Test Methods

Workability of the fresh concrete and compressive strength of the concrete in this research were tested according to the standard ASTM-C143 and BS 1881-116, respectively.

Slump Tests

Table 10 represents the workability of LWAC, GPLWAC, GSLWAC and PSLWAC mixtures. The slump results showed that the fiber added into LWAC decrease the workability specimens.

Mechanical Properties

Table 10 shows the compressive strength results on the base BS 1881-116. For each specimen mixture proportion, three 150 mm × 150 mm × 150 mm cube samples were constructed for compressive strength test and all the mechanical property tests were performed for 28 days. The testing machine with a maximum load capacity of 2000 kN.

TEST SETUP AND PROCEDURE

The specimens was tested under the four-point bending, with 1500 mm (length), 200 mm (depth), 100 mm (width) and a shear span of 550 mm. All the beams had a 50 mm overhang in each side and distance between point loads was 300 mm. Two FRP bars were utilized in the lower part (bottom reinforcement) of each beam; these bars were glass FRP (GFRP) bars with size of 8 or 10 mm. Hence, approximately, the effective depths of the beams with the #8 and #10 mm bars were 170 mm (concrete cover was 30 mm). The one steel bar was utilized in the upper part (top reinforcement) and the φ6@7.5 cm steel stirrups were used along 55 cm at each end of the beams. Furthermore, in the middle part of beams, φ6@15 cm steel stirrups were used. The eight beams were constructed with different flexural

reinforcement ratios. Details and designations all beams are presented in Table 11 and Figure 4, respectively. To investigate the flexural performance of GPLWAC, GSLWAC and PSLWAC concrete beams reinforced with GFRP bar, the four-point static bending test was employed. Figure 5 represents the test setup and schematic diagram**.**

Table 9. Mixture proportions of LWAC, GFLWAC, PFLWAC and SFLWAC

Name of specimen	C (kg/m^3)	W (kg/m^3)	S (kg/m^3)	LECA (kg/m^3)	Silica fume (kg/m^3)	SP (kg/m^3)	Fiber volume fraction (%)		
							GF	PF	SF
LAWC	500	195	265	685	15	5	0	0	0
GFLAWC	500	195	265	685	15	5	0.3	0	0
PFLAWC	500	195	265	685	15	5	0	0.8	0
SFLAWC	500	195	265	685	15	5	0	0	0.25

C: is cement, W: is mixing water, S: is sand, LECA: is light expanded clay aggregate, SP: is super plasticizer, GF: is micro glass fiber, PF: is micro polypropylene fiber, SF: is macro steel fiber, LAWC: is lightweight aggregate concrete, GFLAWC: is micro glass fiber into the LAWC mix, PFLAWC: is micro polypropylene fiber into the LAWC mix and SFLAWC: is macro steel fiber into the LAWC mix.

Table 10. Results of compressive strength, oven dry density and slump tests for specimen LWAC, GFLWAC, PFLWAC and SFLWAC

Name of specimen	Compressive strength (MPa)		Oven dry density (kg/m^3)	Slump (mm)
LWAC	36 35 34	35	1530	100
GFLWAC	37.5 35 36	37	1552	75
PFLWAC	37 35.5 35	35.5	1541	70
SFLWAC	46 45 44	45	1673	50

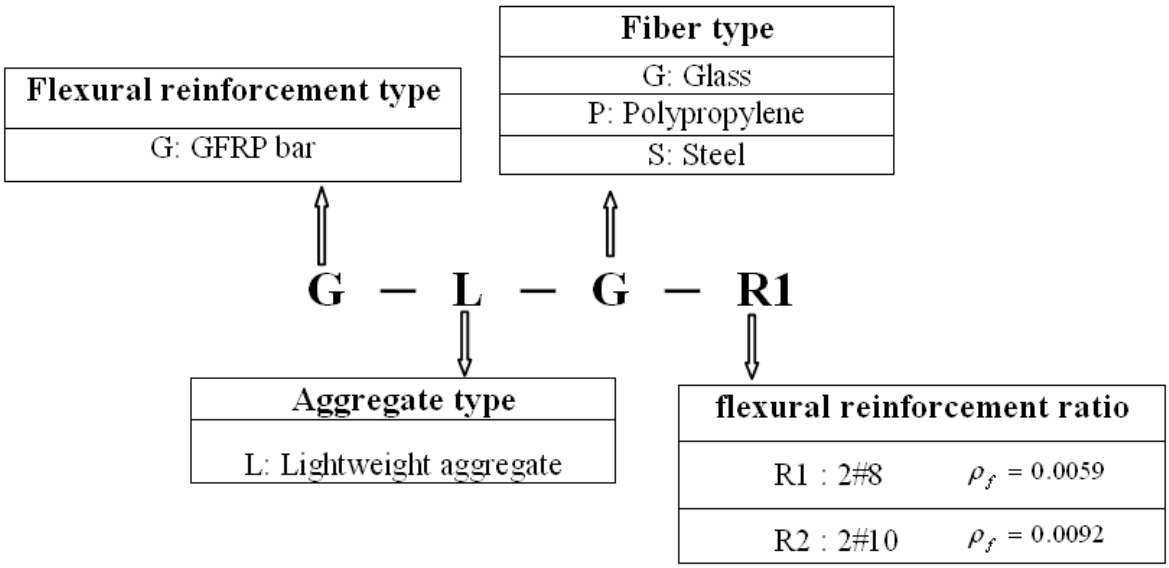

Fig. 4. Designation of the test beams

Table 11. Beam details

Beam code	Concrete type	Beam code	Beam dimensions Width (mm)	Depth (mm)	Effective span (mm)	Bottom reinforcement (GFRP bars)	Top reinforcement (steel bar)	Stirrups (steel)
G-L-R1	LWAC	G-L-R1	100	200	1400	2#8	1φ8	φ6@7.5cm
G-L-R2	LWAC	G-L-R2	100	200	1400	2#10	1φ8	φ6@7.5cm
G-L-G-R1	GFLWAC	G-L-G-R1	100	200	1400	2#8	1φ8	φ6@7.5cm
G-L-G-R2	GFLWAC	G-L-G-R2	100	200	1400	2#10	1φ8	φ6@7.5cm
G-L-P-R1	PFLWAC	G-L-P-R1	100	200	1400	2#8	1φ8	φ6@7.5cm
G-L-P-R2	PFLWAC	G-L-P-R2	100	200	1400	2#10	1φ8	φ6@7.5cm
G-L-S-R1	SFLWAC	G-L-S-R1	100	200	1400	2#8	1φ8	φ6@7.5cm
G-L-S-R2	SFLWAC	G-L-S-R2	100	200	1400	2#10	1φ8	φ6@7.5cm

(a)

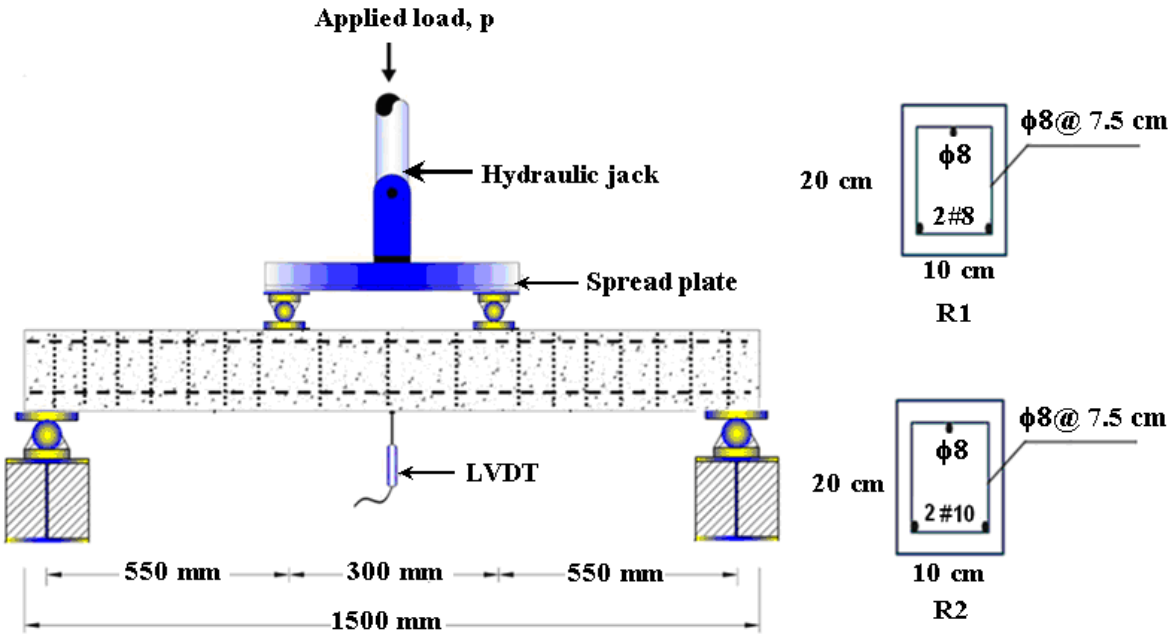

(b)

Fig. 5. Schematic of the four-point static bending test: a) Actual test setup, b) The schematic test set up and two different types of the beam section

TEST RESULTS AND DISCUSSION

The experimental results are summarized of the failure mode, load-deflection behavior, flexural capacity, energy absorbed and ductility of the tested all beams.

Mode of Failure

Table 12 represents the failure modes of the tested beams. The observed failure modes of the evaluated beams are presented in Table 12. Figure 6 shows the final situation of the beams constructed by the pure LWAC. Figures 7-9 illustrate the final situation of the GFLWAC, PFLWAC and SFLWAC specimens, respectively. As depicted in Figures 6, 7b, 8b and 9, the concrete crushing (CC) failure mode for the LWAC, GFLWAC, PFLWAC and SFLWAC was appeared in the compression zone. It is noteworthy that the ACI440.1R-06 code recommends this failure mode for any FRP bars reinforced concrete beams. Since this failure type is less brittle, less catastrophic and more gradual with higher deformability in comparison with the FRP bars' tensile rupture (Kakizawa et al., 1993; Taly et al., 2006; Omar et al., 2019). From Figures 7a and 8a, which present GFRP rupture (GR) failure mode, it is observed that in G-L-G-R1 and G-L-P-R1 beams an increase in balanced reinforcement ratio of the GFRP bars (ρ_{fb}) from 0.9 to 1.4 changed failure mode of GFLWAC and PFLWAC from GR to the CC. The balanced FRP reinforcement ratio can be computed from Eq. (1), and parameters f_{fu}, E_f used of Table 7 also FRP reinforcement ratio can be computed from Eq. (2) on the base ACI 440.1R-06.

$$\rho_{fb} = 0.85\beta_1 \frac{f_c}{f_{fu}} \times \frac{E_f \varepsilon_{cu}}{E_f \varepsilon_{cu} + f_{fu}} \quad (1)$$

where β_1: is the factor taken as 0.85 for concrete strength fc' up to and including 28 MPa. For strength above 28 MPa, this factor is reduced continuously at a rate of 0.05 per each 7 MPa of strength in excess of 28 MPa, but is not taken less than 0.65.

$$\rho_f = \frac{A_f}{bd} \quad (2)$$

where ρ_f : is the FRP reinforcement ratio, A_f: is area of FRP reinforcement, (mm^2), b: is width of rectangular cross section, (mm) and d: is distance from extreme compression fiber to centroid of tension reinforcement, (mm).

Table 12. Test results and failure modes

Beam code	Compressive strength (MPa)	β_1	ε_{cu}	Reinforcement ratio (ρ_f/ρ_{fb})%	Ultimate load (kN)	Mid-section displacement at (mm)	Failure modes	ACI failure consistency
G-L-R1	35	0.85	0.003	0.9	18.62	16.64	C.C	-
G-L-G-R1	37	0.842	0.0029	0.9	26.97	32.25	G.R	✓
G-L-P-R1	35.5	0.839	0.0029	0.9	24.52	42.84	G.R	✓
G-L-S-R1	45	0.778	0.0024	0.9	39.24	43.78	C.C	-
G-L-R2	35	0.85	0.003	1.4	27.46	14.5	C.C	✓
G-L-G-R2	37	0.842	0.0029	1.4	37.76	27.56	C.C	✓
G-L-P-R2	35.5	0.839	0.0029	1.4	30.41	35.09	C.C	✓
G-L-S-R2	45	0.778	0.0024	1.4	48.55	43.14	C.C	✓

ρ_f: is FRP reinforcement ratio, ρ_{fb}: is GFRP reinforcement ratio producing balanced strain conditions, ε_{cu}: is ultimate strain in concrete, C.C: is concrete crushing, G.R: is GFRP bars rupture.

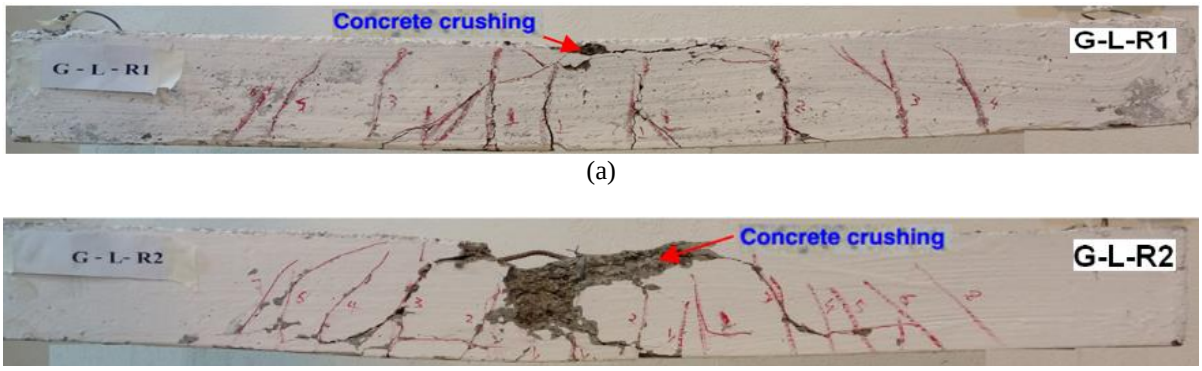

Fig. 6. Modes of failure in the specimens G-L-R1 and G-L-R2: a) Concrete crushing failure specimen G–L–R1, b) Concrete crushing failure Specimen G–L–R2

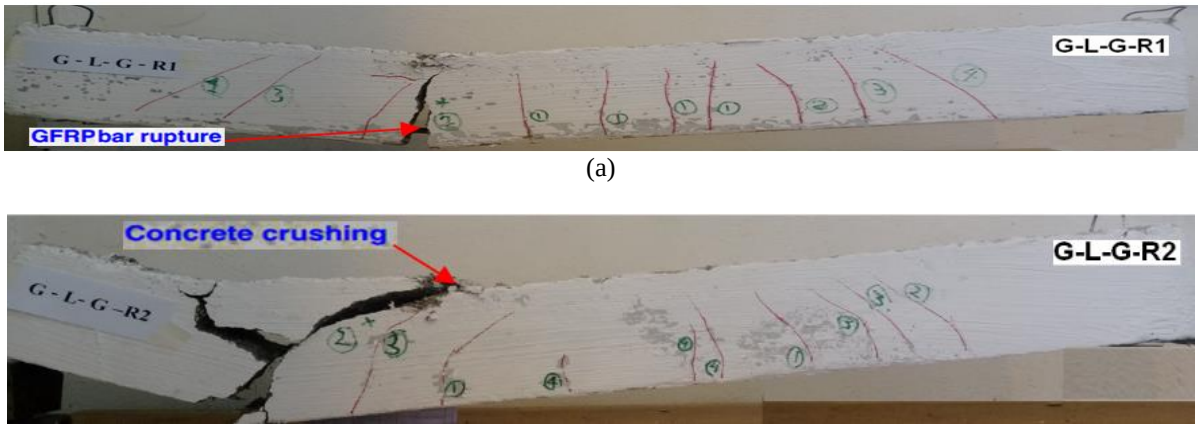

Fig. 7. Modes of failure in specimens G-L-G-R1 and G-L-G-R2: a) Rupture of GFRP reinforcement bars specimen G–L–G–R1, b) Concrete crushing failure specimen G–L–G–R2

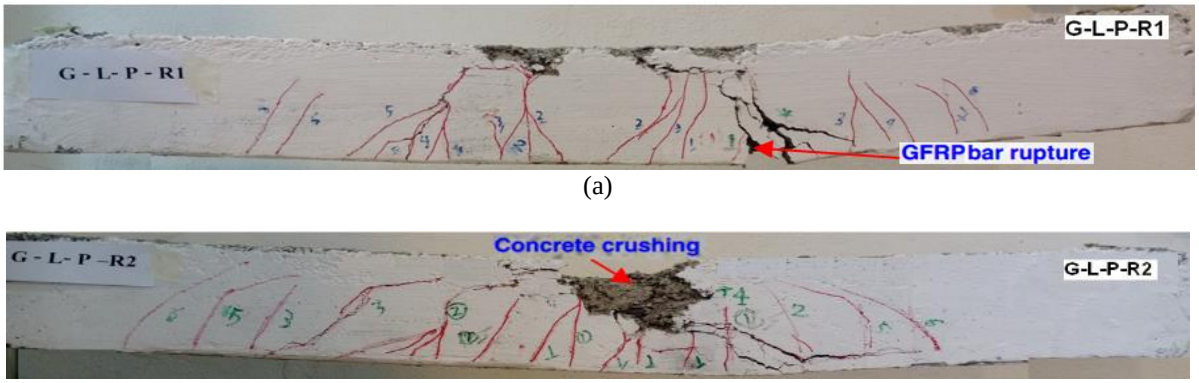

Fig. 8. Modes of failure in specimens G-L-P-R1 and G-L-P-R2: a) Rupture of GFRP reinforcement bars specimen G–L–P–R1, b)Concrete crushing failure specimen G–L–P–R2

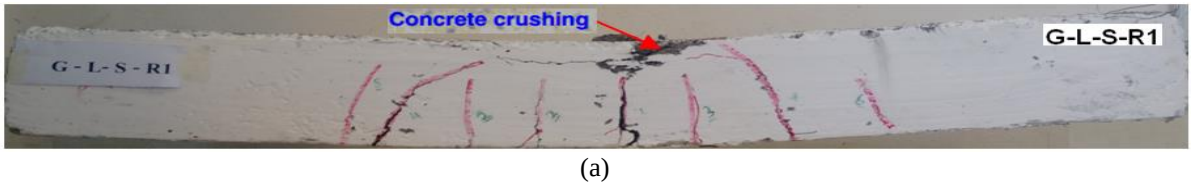

(b)

Fig. 9. Modes of failure in specimens G-L-S-R1 and G-L-S-R2: a) Concrete crushing failure specimen G–L–S–R1, b) Concrete crushing failure specimen G–L–S–R2

Load-Deflection Behavior

The experimental load to mid-span deflection curves and ultimate loads of the GFRP reinforced LWAC, GFLWAC, PFLWAC and SFLWAC beams are shown in Figures 10 and 11, respectively. Each curve shows the mid-span deflection at beam was obtained by the LVDT. As can be seen, added fibers caused an increase in the ductility of the beams, significantly, which were reinforced by $1.4\rho_{fb}$ GFRP bars. Figures 10a-10c show that reinforcement ratio increases from $0.9\rho_{fb}$ to $1.4\rho_{fb}$ in LWAC, GFLWAC, PFLWAC, and SFLWAC increase the ultimate load by 47%, 40%, 24% and 23%, respectively.

The corresponding of the first crack in the beams is shown in Figure 12. The first crack is increased by adding fiber to LWAC. Fiber's bridging between boundaries the micro-cracks delays crack growth in LWAC, it also increases the tensile strength of concrete, which is directly affects the ultimate capacity of beam. In all fiber-added specimens, the cracking-load is greater than the without fiber beam (reference). The first cracking of G-L-G-R1, G-L-P-R1 and G-L-S-R1 are respectively 45%, 54% and 45% greater than the G-L-R1 first cracking load, while the first cracking load of the G-L-G-R2, G-L-P-R2 and G-L-S-R2 are respectively 32%, 40% and 34% greater than the capacity of G-L-R2 first cracking load.

Second section of the load-deflection curves shows the cracked beams' behavior and reduction in its stiffness. In reference beams without fiber, the small number of cracks formed with wide width. In sample beams with fiber, the micro-cracks formed and the number of low width cracks increases by increase in loading. The use of SF in the sample beams makes the slope of this region steeper. As can be seen, added fibers caused significant increase in the ductility of the beams.

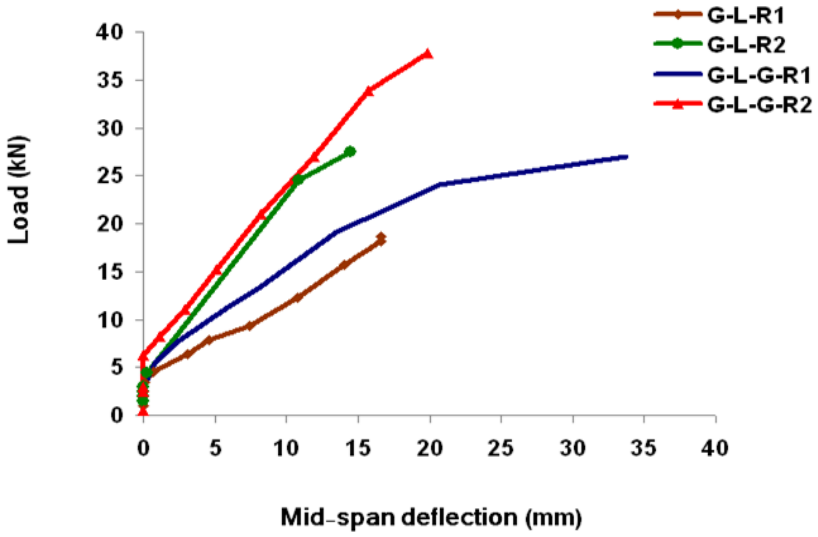

(a)

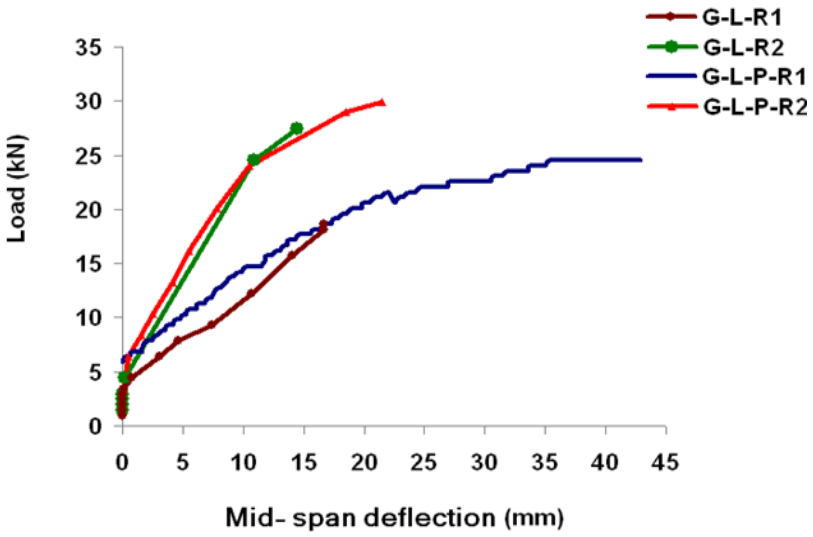
G-L-R1
G-L-R2
G-L-P-R1
G-L-P-R2
Load (kN)
Mid- span deflection (mm)

(b)

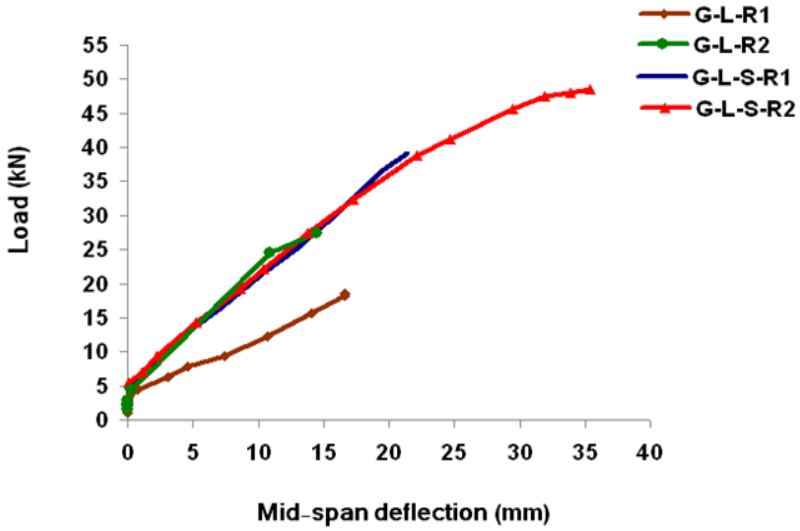
G-L-R1
G-L-R2
G-L-S-R1
G-L-S-R2
Load (kN)
Mid-span deflection (mm)

(C)

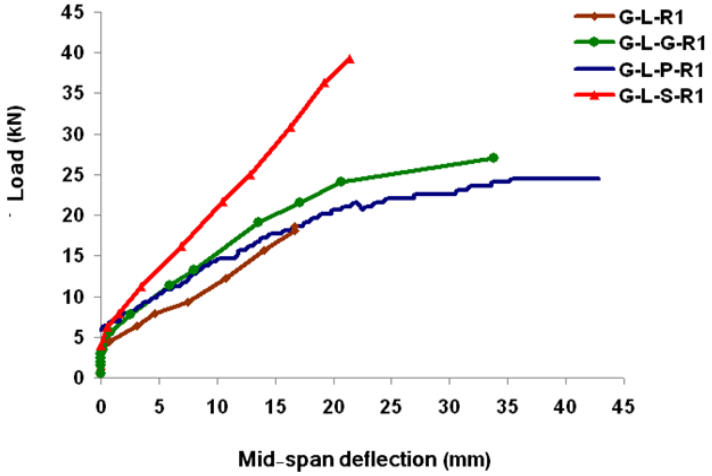
G-L-R1
G-L-G-R1
G-L-P-R1
G-L-S-R1
Load (kN)
Mid-span deflection (mm)

(d)

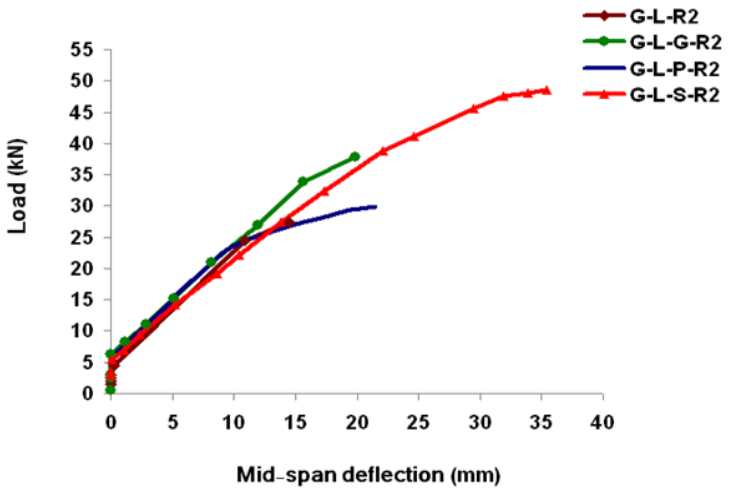

(e)

Fig. 10. Load-deflection: a) Beam code: G-L-R1, G-L-R2, G-L-G-R1 and G-L-G-R2, b) Beam code: G-L-R1, G-L-R2, G-L-P-R1 and G-L-P-R2, c) Beam code: G-L-R1, G-L-R2, G-L-S-R1 and G-L-S-R2, d) Beam code: G-L-R1, G-L-G-R1, G-L-P-R1 and G-L-S-R1, e) Beam code: G-L-R2, G-L-G-R2, G-L-P-R2 and G-L-S-R2

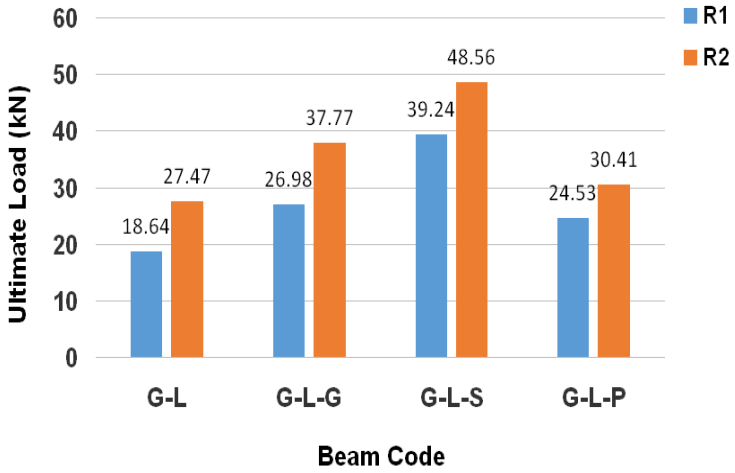

Fig. 11. Ultimate load

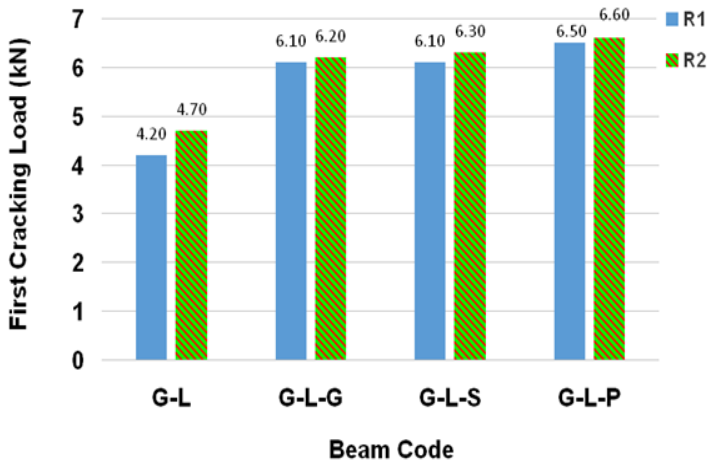

Fig. 12. First cracking load

Ductility

Figure 10d depicts that the ductility of the G-L-P-R1, G-L-S-R1 and G-L-G-R1 beams increases to 7.21, 6.29 and 5.7, respectively. Figure 10e shows the ductility of the G-L-P-R2, G-L-S-R2 and G-L-G-R2 beams increases to 8.27, 6.78 and 4.97, respectively.

Flexural Capacity

The flexural capacity depends on whether CC or FRP rupture modes govern the failure in an FRP reinforced member (ACI 440.1R-06). Failure modes of the beams and their nominal flexural strength can be determined by ACI 440.1R-06 and ISIS design manual No. 3 and it could be compared with the test findings have been shown in Table 12. ACI 440.1R-06 and ISIS Canadian code are provided for pure LWAC and they do not have any comments for fiber added LWAC. Therefore, we calculated a strength factor for the flexure capacity (Ψ) for matching the code nominal calculated strength (for pure LWAC) with the experimental results (for fiber added LWAC). Table 13 shows the results of Ψ factor for different added fiber materials matching to the design codes. As can be seen, the ratio of M_{exp}/Mn_{ACI} is less than 1 for five beams G-L-R1, G-L-R2, G-L-P-R1, G-L-P-R2 and G-L-G-R2 and also ratio of M_{exp}/Mn_{ISIS} is less than 1 for four beams G-L-R1, G-L-R2, G-L-G-R2 and G-L-P-R2.

Energy Absorption Capacity

The capacities of energy absorption of the beams were measured as the area surrounded by the load-deflection curve. Figure 13 displays the capacity of energy absorption of all eight beams. This figure shows that the beams made of added fiber into the LWAC have much more energy absorption capacity compared to the pure LWAC beams. The capacities of the specimens of G-L-S-R1, G-L-G-R1 and G-L-P-R1 are respectively 2.40, 2.50 and 3.35 times greater than the capacity of G-L-R1 while the capacities of the specimens of G-L-P-R2, G-L-G-R2 and G-L-S-R2 are respectively 1.71, 1.87 and 4.0 times greater than the capacity of G-L-R2.

CONCLUSIONS

In this research, laboratory tests were conducted for the assessment of lightweight fiber concrete beams reinforced GFRP (glass fiber reinforced polymer) bars. The results indicted that the behavior of the beams depends on the reinforcement ratios and the fibers types. According to the experimental results, the main conclusions are given as below:

Table 13. Comparisons between the nominal flexural strength calculated by design codes for pure LWAC and the experimental capacities of the fiber added into LWAC mix

Beam code	$M_{exp}(kN.m)$	$Mn_{ACI}(kN.m)$	$Mn_{ISIS}(kN.m)$	Ψ	
				(M_{exp}/Mn_{ACI})	(M_{exp}/Mn_{ISIS})
G-L-R1	5.12	7.41	6.12	0.69	0.84
G-L-R2	7.55	11.81	11.84	0.64	0.64
G-L-G-R1	7.41	7.41	6.12	1	1.21
G-L-G-R2	10.38	11.8	11.84	0.88	0.88
G-L-P-R1	6.74	7.41	6.12	0.91	1.10
G-L-P-R2	8.36	11.81	11.84	0.71	0.71
G-L-S-R1	10.79	7.41	6.12	1.46	1.76
G-L-S-R2	13.35	11.81	11.84	1.13	1.13

M_{exp}: is experimental flexural capacity , Mn_{ACI}: is nominal flexural strength (ACI 440.1R-06) and Mn_{ISIS}: is nominal flexural strength (ISIS Canada).

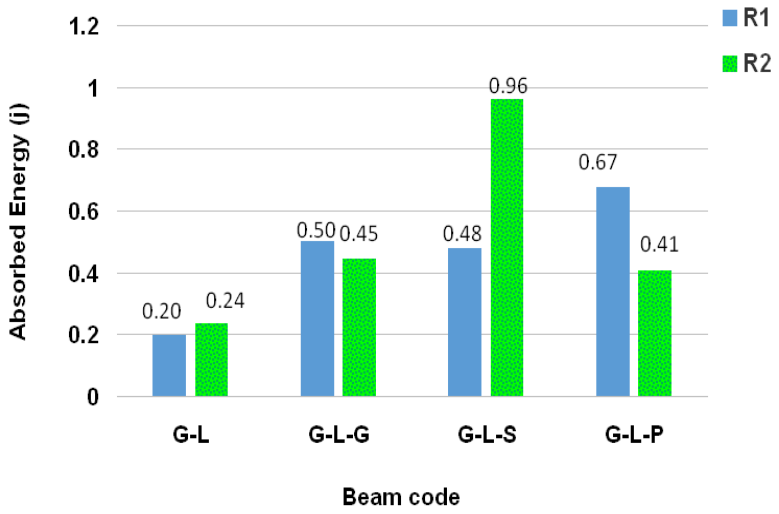

Fig. 13. Energy absorption capacity of beams under static loading

- The GFLWAC and PFLWAC with the reinforcement ratio from of 1.4ρ_{fb} showed better failure mode relative to the pure LWAC and SFLWAC (macro Steel Fiber (SF) into the LWAC). Increase of the reinforcement ratio from 0.9ρ_{fb} to 1.4ρ_{fb} in specimen beams made of GFLWAC (micro glass fiber (GF) into the LWAC) and PFLWAC (micro polypropylene fiber (PF) into the LWAC) caused the failure mode changes from GR to CC while the failure modes for pure LWAC and SFLWAC remain the same in CC mode.
- The maximum ultimate loads for specimen beams achieved with the reinforcement ratio of 1.4ρ_{fb}, and the ultimate loads increased up to 47%, 40%, 24% and 23%, respectively for SFLWAC, PFLWAC, and GFLWAC specimen beams when reinforcement ratio increased from 0.9ρ_{fb} to 1.4$\rho_{fb.}$
- Adding GF, PF and SF into the LWAC mixture caused a noticeable increase in the first cracking moment and that is more efficient for lower reinforced beams. As the reinforcement ratio of GFRP bars increased from 0.9ρ_{fb} to 1.4ρ_{fb}, the first cracking load of the specimen beams increased by 45% and 32% by adding GF, 54% and 40% by adding PF and 45% and 34% by adding SF.
- Flexural capacity comparing factor (Ψ) calculated from M_{exp}/Mn_{ACI} and M_{exp}/Mn_{ISIS} shown the efficiency of the added fibers into the LWAC material. The Ψ factor for SF is almost 1.5 times to the Ψ factor for GF and PF.
- Energy absorption increased by adding fibers into the LWAC material. The best results were obtained for specimens SFLWAC reinforced with 0.9ρ_{fb} and 1.4ρ_{fb}, which was 2.40 and 4.0 times greater than beams without added fibers, respectively. Other fibers also showed an increase in energy absorption such that the GFLWAC and PFLWAC reinforced with 0.9ρ_{fb} presented 2.50 and 3.35-time increase while GFLWAC and PFLWAC reinforced with 1.4ρ_{fb} showed 1.87 and 1.71-time increases compared to beams without added fibers.
- Adding fibers to the LWAC can significantly increase the ductility relative to the specimens without added fibers. Ductility increased by 3.92, 3.29 and 3.05 for specimen beams made with PFLWAC, SFLWAC and GFLWAC reinforced with 0.9ρ_{fb}, respectively and increased up to 4.13, 3.35 and 3.14 times for specimen beams made with SFLWAC, GFLWAC and PFLWAC and reinforced with 1.4ρ_{fb}, respectively.
- The cost of fiber added lightweight aggregate concrete mixture is estimated about 5 to 20 percent more than the normal lightweight concrete. This extra cost seems

reasonable in compare with the behavioral advantages of this material. While the lightweight aggregate concrete and GFRP bars are both relatively brittle materials and the use of GF, PF and SF with those materials showed more ductile and softer flexural behavior, the use of fiber added LWAC mixture is recommendable.

REFERENCES

American Concrete Institute (ACI). (2003).*Guide for structural lightweight-aggregate concrete*, ACI 213R–03 Farmington Hills, MI.

American Concrete Institute. Committee 440. (2006), *Guide for the design and construction of structural concrete reinforced with FRP bars*, ACI 440.1 R-06.

ASTM Standard (2015), *Standard test method for slump of hydraulic-cement concrete*, ASTM Annual Book of ASTM Standards C143.

Badogiannis, E.G., Christidis, K.I. and Tzanetatos, G.E. (2019). "Evaluation of the mechanical behavior of pumice lightweight concrete reinforced with steel and polypropylene fibers", *Construction and Building Materials*, 196, 443-456.

Bilodeau, A., Kodur, V.K.R. and Hoff, G.C. (2004). "Optimization of the type and amount of polypropylene fibers for preventing the spalling of lightweight concrete subjected to hydrocarbon fire", *Cement and Concrete Composites*, 26(2), 163-174.

Bogas, J.A. and Gomes, A. (2015). "Non-steady-state accelerated chloride penetration resistance of structural lightweight aggregate concrete", *Cement and Concrete Composites*, 60, 111-122.

Campione, G. and La Mendola, L. (2004). "Behavior in compression of lightweight fiber reinforced concrete confined with transverse steel reinforcement", *Cement and Concrete Composites*, 26(6), 645-656.

Chen, B. and Liu, J. (2005). "Contribution of hybrid fibers on the properties of the high-strength lightweight concrete having good workability", *Cement and Concrete Research*, 35(5), 913-917.

Choi, J., Zi, G., Hino, S., Yamaguchi, K. and Kim, S. (2014). "Influence of fiber reinforcement on strength and toughness of all-lightweight concrete", *Construction and Building Materials*, 69, 381-389.

Domagała, L. (2011). "Modification of properties of structural lightweight concrete with steel fibres", *Journal of Civil Engineering and Management*, 17(1), 36-44.

Guler, S. (2018). "The effect of polyamide fibers on the strength and toughness properties of structural lightweight aggregate concrete", *Construction and Building Materials*, 173, 394-402.

Hamoush, S., Abu-Lebdeh, T. and Cummins, T. (2010). "Deflection behavior of concrete beams reinforced with PVA micro-fibers", *Construction and Building Materials*, 24(11), 2285-2293.

ISIRI (Institute of Standards and Industrial Research of Iran). (2000). *Specification for Portland cement*, ISIRI Number 389, 8th Edition.

ISIS, D.M.N. (2007). "Reinforcing concrete structures with fiber reinforced polymers", *Intelligent Sensing for Innovative Structures Canada*, Winnipeg.

Jun Li, J., Jun Wan, C., gang Niu, J., feng Wu, L. and chao Wu, Y. (2017). "Investigation on flexural toughness evaluation method of steel fiber reinforced lightweight aggregate concrete", *Construction and Building Materials*, 131, 449-458.

Kakizawa, T., Ohno, S. and Yonezawa, T. (1993). "Flexural behavior and energy absorption of carbon FRP reinforced concrete beams", *Special Publication*, 138, 585-598.

Kara, I., Ashour, A., Körog˘lu, A. (2015). "Flexural behavior of hybrid FRP/steel reinforced concrete beams", *Composite Structures*, 129, 111–121.

Khaloo, A., Raisi, E.M., Hosseini, P. and Tahsiri, H. (2014). "Mechanical performance of self-compacting concrete reinforced with steel fibers", *Construction and Building Materials*, 51, 179-186.

Lee, J.H., Cho, B. and Choi, E. (2017). "Flexural capacity of fiber reinforced concrete with a consideration of concrete strength and fiber content", *Construction and Building Materials*, 138, 222-231.

Li, J., Niu, J., Wan, C., Liu, X. and Jin, Z. (2017). "Comparison of flexural property between high performance polypropylene fiber reinforced lightweight aggregate concrete and steel fiber reinforced lightweight aggregate concrete", *Construction and Building Materials*, 157, 729-736.

Libre, N.A., Shekarchi, M., Mahoutian, M. and Soroushian, P. (2011). "Mechanical properties of hybrid fiber reinforced lightweight aggregate concrete made with natural pumice", *Construction and Building Materials*, 25(5), 2458-2464.

Lin, C., Kayali, O., Morozov, E.V. and Sharp, D.J. (2014). "Influence of fiber type on flexural behaviour of self-compacting fiber reinforced cementitious composites", *Cement and Concrete Composites*, 51, 27-37.

Oktay, H., Yumrutaş, R. and Akpolat, A. (2015). "Mechanical and thermo physical properties of

lightweight aggregate concretes", *Construction and Building Materials*, 96, 217-225.

Omar, A., Ehab, A., Hamdy, M. and Brahim, B. (2019). "Flexural strength and serviceability evaluation of concrete beams reinforced with deformed GFRP bars", *Engineering Structures*, 186, 282-296.

Qian, C.X. and Stroeven, P. (2000). "Development of hybrid polypropylene-steel fiber-reinforced concrete", *Cement and Concrete Research*, 30(1), 63-69.

Ramezani, A.R. and Esfahani, M.R. (2018). "Evaluation of hybrid fiber reinforced concrete exposed to severe environmental conditions", *Civil Engineering Infrastructures Journal*, 51(1), 119-130.

Shafigh, P., Jumaat, M.Z., Mahmud, H.B. and Alengaram, U.J. (2011). "A new method of producing high strength oil palm shell lightweight concrete", *Materials and Design*, 32(10), 4839-4843.

Standard BS (1983). *Method for determination of compressive strength of concrete cubes concrete specimens*, BS, 1881-116.

Tajra, F., Elrahman, M., Lehmann, C., Stephan, D. (2019). "Properties of lightweight concrete made with core-shell structured lightweight aggregate", *Construction and Building Materials*, 205, 39-51.

Taly, N., Ganga, H.V. and Vijay, P.V. (2006). *Reinforced concrete design with FRP composites*, CRC press.

Tang, W.C., Balendran, R.V., Nadeem, A. and Leung, H.Y. (2006). "Flexural strengthening of reinforced lightweight polystyrene aggregate concrete beams with near-surface mounted GFRP bars", *Building and Environment*, 41(10), 1381-1393.

Vakili, S.E., Homami, P. and Esfahani, M.R. (2019). "Effect of fibers and hybrid fibers on the shear strength of lightweight concrete beams reinforced with GFRP bars", *In Structures*, 20, 290-297, Elsevier.

Wu, T., Yang, X., Wei, H., Liu. (2019). "Mechanical properties and microstructure of lightweight aggregate concrete with and without fibers", *Construction and Building Materials*, 199, 526-539.

Yoon, J.Y., and Kim, J.H. (2019). "Mechanical properties of preplaced lightweight aggregates concrete", *Construction and Building Materials*, 216, 440-449.

Zhu, H., Cheng, S., Gao, D., Neaz, S.M. and Li, C. (2018). "Flexural behavior of partially fiber-reinforced high-strength concrete beams reinforced with FRP bars", *Construction and Building Materials*, 161, 587-597.